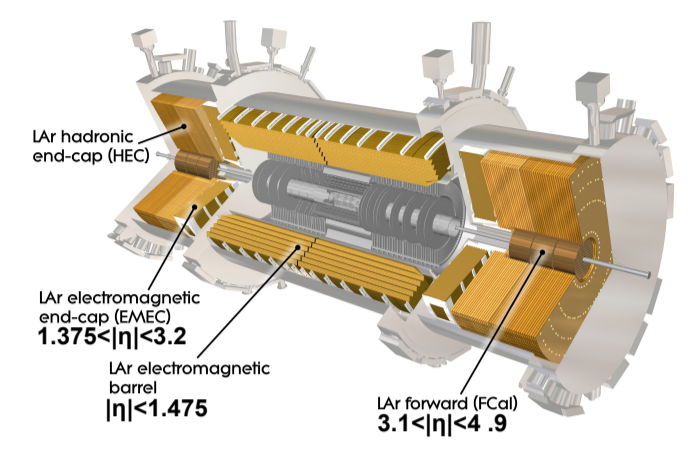


## Operation and performance of the ATLAS liquid argon electromagnetic calorimeters

The electromagnetic calorimeter is a key component for the achievement of the ATLAS physics goals. It must provide an excellent energy resolution in a vast domain (1 GeV – several TeV) as well as great abilities for electron and photon identification. This poster presents the performances reached in the first 3 years of data taking at the LHC.



**Sampling calorimeter** : lead absorbers + liquid argon as ionized medium  
**Accordion structure** : excellent uniformity in  $\phi$   
 Segmentation in precision region ( $|\eta| < 2.5$ ) :

**Back** : correct for shower energy leakage beyond calorimeter  
**Middle** : collect most of shower energy,  $\phi$  measurement  
**Front** : precise  $\eta$  measurement,  $\gamma$ - $\pi^0$  separation  
**Presampler** ( $|\eta| < 1.8$ ) : flat, no absorber control energy losses before calorimeter

**~173k** readout channels, 50% front, 30% middle

### Readout and energy reconstruction

Copper electrodes interleaved with kapton, maintained by honeycomb structure filled with argon

Field electrodes : 2 independent supplying lines to limit the risk of inefficient areas  
 Nominal HV : 2kV in barrel, 1 to 2.5 kV in end-caps because of variable drift gap

Shaping to reduce signal duration (drift time ~450 ns), out-of-time pile-up effect, and total noise

Readout electrode : capacitive coupling

**Front End Board** : fast readout mounted on cryostat, 128 channels/board, 1524 boards

Build trigger towers L1 decision in 2  $\mu$ s    40 MHz sampling    Optical link to back-end  
 2.5  $\mu$ s buffer

Calibration up to 32 samples/event, data-taking 5 samples  
 → limited by L1 rate (75 kHz) and bandwidth

Optimal Filtering Coefficients extracted from calibration

**Forward calorimeter**  $3.1 < |\eta| < 4.9$   
 High particles flux → specific structure  
 Cylindrical electrodes in copper matrix  
 Reduced gap size 269  $\mu$ m

### Stability during operation

**Electronic calibration** performed daily by injecting calibration signal, checking :

- Pedestal and noise (no signal)
- Gain
- Shape → recompute OFCs (weekly)

Stability of pedestals over 2012, all channels:

Very stable **-0.03 ADC**, gain **0.005-0.03%**

### Temperature homogeneity and uniformity

508 monitoring probes in various locations  
 -2%/K change of energy scale (drift speed)  
 → excursions must be kept below 100 mK

Uniformity **~60 mK**, very small excursions  
 → no degradation of energy resolution

**Liquid argon purity**  
 Impurity level must be kept below 1000 ppb  
 Achieve **200 ppb** in barrel, **140 ppb** in end-caps

### Timing

**Signal timing** obtained from sampled shape with different set of OFCs

FEBs aligned at O(100 ps), to be compared with nominal bunch crossing period of 25 ns

Object level (electron) **~300 ps**, including 220 ps beam spread

Application : noise cleaning (e.g. cosmics), long-lived particles

### Data taking efficiency

**ATLAS online recording efficiency** : >94% for 2011+2012  
 → EM calorimeter contribution negligible

**Data quality**: fraction of recorded data good for physics

**Total EM calo DQ losses in 2012** : 0.88% recorded data  
 → used previous years experience (2011 inefficiency 3.3%)

**Operational EM calo fraction**: 99.9% of channels

Trips of HV supply modules responsible for **0.46%**  
 → very noisy environment, unknown HV on electrodes

Reduced wrt 2011 losses (1%) thanks to new HV modules tolerating temporary current overload, avoiding HV trip

Quality factor very valuable tool to spot cell noise

Comparing sampled signal and ref. shapes

Identified by fraction of cells with energy above 3 $\sigma$  (empty bunches) → 109/h  
 Improved by rejecting events with many cells with **bad quality factor** → 12/h  
 Fully cleaned by **time window veto** ( $\pm 250$  ms) around candidates → 3/h  
 Corresponding loss on 2012 data : **~0.2%**  
 Early identification less efficient in 2011, noise bursts caused 1.2% data loss

### Electron and photon reconstruction

Pre-clusters 3x5 middle cells, local  $E_T$  maximum,  $E_T > 2.5$  GeV  
 Track found in  $\Delta\eta \times \Delta\phi = 0.05 \times 0.1$  → **electron**  
 final cluster 3x7 (barrel) or 5x5 (end-cap)  
**No track** → **unconverted photon**  
 final cluster 3x5 (barrel) or 5x5 (end-cap)  
**Track + conversion vertex** → **converted photon**  
 same cluster as electron  
 2012 : refitted tracks with Brehmsstrahlung emission model  
 → improved efficiency, especially low  $E_T$  / high  $\eta$

### Electron and photon identification

EM calorimeter crucial for particle identification

**Discriminant variables** built on shower shape : lateral width, leakage in hadronic layer...

**Jet candidate with a leading  $\pi^0$**

Shower width in middle layer    High granularity in front layer allowing resolution of  $\pi^0$ - $\gamma\gamma$

**Electron ID** further makes use of track quality, track-cluster matching, transition radiation with TR tracker...

Efficient electron ID also in  $2.5 < |\eta| < 4.9$

Electron identification efficiency (%)

Number of reconstructed primary vertices

Unconverted  $\gamma$ ,  $|\eta| < 0.6$   
 Converted  $\gamma$ ,  $|\eta| < 0.6$

### Energy calibration for electrons and photons

**Calorimeter energy resolution:**  

$$\sigma/E_T = a/\sqrt{E_T} \oplus b/E_T \oplus c$$

**a** stochastic term **~10%**  
 Shower particles stopped in absorber

**b** noise, negligible at high  $E_T$   
 Electronic (preamplifiers) + pile-up

**c** constant term, design **0.7%**  
 Inhomogeneities in cell geometry, or temperature, material in front of calorimeter, local mis-calibration

**Cluster calibration** corrects for fine geometry effects and accounts for various losses :

**E** =  $E_{front}$  Material in front of calorimeter  
 +  $E_{calo}$  Cluster + out-of-cluster  
 +  $E_{back}$  Longitudinal leak in hadronic calorimeter

Contributions parametrized by functions of  $\eta$ , longitudinal barycenter, and fraction of energy in presampler  
 Simulation used to tune parametrization, using dedicated samples recording energy deposits in all passive detector material

**Angular resolution**(design):  $\Delta\eta \sim 3 \cdot 10^{-4}$ ,  $\Delta\phi \sim 1$  mrad    Future gains by improved material mapping

**Absolute energy scale** determined *in situ* from reconstructed Z → ee invariant mass  
 Cross-check :  $W \rightarrow e\nu$  (E/p),  $J/\psi$  (low energy)

Scale corrections **~2%** barrel, **~4%** end-caps

**Excellent stability** regarding pile-up and time :

**Energy resolution** also measured from Z peak

Subsystem	$\eta$ -range	Effective constant term, $c_{data}$
EMB	$ \eta  < 1.37$	$1.2\% \pm 0.1\%$ (stat) $+0.5\%$ (syst)
EMEC-OW	$1.52 <  \eta  < 2.47$	$1.8\% \pm 0.4\%$ (stat) $\pm 0.4\%$ (syst)
EMEC-IW	$2.5 <  \eta  < 3.2$	$3.3\% \pm 0.2\%$ (stat) $\pm 1.1\%$ (syst)
FCal	$3.2 <  \eta  < 4.9$	$2.5\% \pm 0.4\%$ (stat) $+1.0\%$ (syst)

### Implication in Higgs boson mass measurement

Particularly important in  $H \rightarrow \gamma\gamma$  search :

- **Large background** ( $jj+\gamma\gamma$ ) requires excellent photon ID
- **Narrow invariant mass resonance** needed to disentangle signal from continuous irreducible background
- excellent energy resolution
- excellent angular resolution, achieved in particular by vertex pointing with front and middle layer cluster barycenters

Photon energy scale uncertainty **0.55%**, main contribution to mass measurement  
 → negligible vertex contribution to invariant mass resolution (overall 1.7 GeV)

$H \rightarrow 4e$  requires high efficiency electron ID, and good energy resolution

Selected diphoton sample

Events / 2 GeV

Events - Fitted bkg

→ Photon energy scale uncertainty **0.55%**, main contribution to mass measurement  
 → negligible vertex contribution to invariant mass resolution (overall 1.7 GeV)

$H \rightarrow 4e$  requires high efficiency electron ID, and good energy resolution